


SHORT REPORT

Open Access



A dual tracer [^{11}C]PBR28 and [^{18}F]FDG microPET evaluation of neuroinflammation and brain energy metabolism in murine endotoxemia

Santhoshi P. Palandira^{1†}, Joseph Carrion^{1†}, Lauren Turecki¹, Aidan Falvey¹, Qiong Zeng¹, Hui Liu¹, Tea Tsaava¹, Dov Herschberg¹, Michael Brines¹, Sangeeta S. Chavan^{1,2}, Eric H. Chang^{1,2}, An Vo^{1,2}, Yilong Ma^{1,2}, Christine N. Metz^{1,2}, Yousef Al-Abed^{1,2}, Kevin J. Tracey^{1,2} and Valentin A. Pavlov^{1,2*} 

Abstract

Background: Brain metabolic alterations and neuroinflammation have been reported in several peripheral inflammatory conditions and present significant potential for targeting with new diagnostic approaches and treatments. However, non-invasive evaluation of these alterations remains a challenge.

Methods: Here, we studied the utility of a micro positron emission tomography (microPET) dual tracer ([^{11}C]PBR28 – for microglial activation and [^{18}F]FDG for energy metabolism) approach to assess brain dysfunction, including neuroinflammation in murine endotoxemia. MicroPET imaging data were subjected to advanced conjunction and individual analyses, followed by post-hoc analysis.

Results: There were significant increases in [^{11}C]PBR28 and [^{18}F]FDG uptake in the hippocampus of C57BL/6J mice 6 h following LPS (2 mg/kg) intraperitoneal (i.p.) administration compared with saline administration. These results confirmed previous postmortem observations. In addition, patterns of significant simultaneous activation were demonstrated in the hippocampus, the thalamus, and the hypothalamus in parallel with other tracer-specific and region-specific alterations. These changes were observed in the presence of robust systemic inflammatory responses manifested by significantly increased serum cytokine levels.

Conclusions: Together, these findings demonstrate the applicability of [^{11}C]PBR28 - [^{18}F]FDG dual tracer microPET imaging for assessing neuroinflammation and brain metabolic alterations in conditions “classically” characterized by peripheral inflammatory and metabolic pathogenesis.

Keywords: Murine endotoxemia, Brain, Neuroinflammation, MicroPET imaging, Microglia, Brain metabolism, Conjunction analysis, [^{11}C]PBR28, [^{18}F]FDG

Background

Brain neuronal dysfunction and neuroinflammation (inflammation in the central nervous system, CNS) are traditionally attributed to Alzheimer’s disease and other neurodegenerative diseases (Heneka et al, 2015; Metz & Pavlov, 2021; Streit et al, 2004; Leng & Edison, 2021). However, brain dysfunction, including

[†]Santhoshi P. Palandira and Joseph Carrion contributed equally to this work.

*Correspondence: vpavlov@northwell.edu

² Donald and Barbara Zucker School of Medicine at Hofstra/Northwell, Hempstead, NY, USA

Full list of author information is available at the end of the article



© The Author(s) 2022. **Open Access** This article is licensed under a Creative Commons Attribution 4.0 International License, which permits use, sharing, adaptation, distribution and reproduction in any medium or format, as long as you give appropriate credit to the original author(s) and the source, provide a link to the Creative Commons licence, and indicate if changes were made. The images or other third party material in this article are included in the article’s Creative Commons licence, unless indicated otherwise in a credit line to the material. If material is not included in the article’s Creative Commons licence and your intended use is not permitted by statutory regulation or exceeds the permitted use, you will need to obtain permission directly from the copyright holder. To view a copy of this licence, visit <http://creativecommons.org/licenses/by/4.0/>.

neuroinflammation has been also documented in conditions “classically” characterized by peripheral immune and metabolic dysregulation, including endotoxemia and sepsis (Pavlov & Tracey, 2015). Endotoxemia, induced by peripheral lipopolysaccharide (LPS) administration provides a standardized model to study innate immune responses and the cardiometabolic effects of systemic cytokine release and inflammation both in animals and humans (Patel et al, 2015; Buras et al, 2005). Endotoxemia has been also used to study immune and cardiometabolic dysregulation with some relevance to sepsis - a devastating condition defined as life-threatening organ dysfunction caused by a dysregulated host response to infection (Singer et al, 2016). The brain is profoundly affected in endotoxemia, and sepsis, and *sepsis associated encephalopathy* - a severe brain dysfunction caused by systemic inflammation in the absence of direct brain infection, has been documented (Gofton & Young, 2012; Meneses et al, 2019). Sepsis associated encephalopathy is linked to significantly higher mortality and early diagnosis is key for improving the outcome (Gofton & Young, 2012; Sprung et al, 1990). Among other factors in the brain, neuroinflammation and metabolic derangements contribute to the development of sepsis associated encephalopathy (Gofton & Young, 2012; Meneses et al, 2019). Therefore, real time evaluation of brain function using non-invasive approaches in these conditions is important for designing new diagnostic approaches and evaluation of current and potential treatments within the scope of Bioelectronic Medicine (Pavlov & Tracey, 2022).

Positron emission tomography (PET) provides a non-invasive approach for imaging the brain and studying functional alterations including neuroinflammation and altered energy metabolism in disease settings. Microglia are a major cell type with immune function in the CNS/brain and a key driver of neuroinflammation (Streit et al, 2004). Astrocytes, the most abundant cell type in the CNS/brain also have key roles in neuroinflammation (Giovannoni & Quintana, 2020). Microglia and astrocytes provide structural, trophic, and metabolic support to neurons and are active modulators of neuronal synaptic interaction and neuronal plasticity; changes in microglia and astrocyte functional states can result in neuronal synaptic reorganization, impaired neuronal survival and altered brain function (Garden & Möller, 2006; Hanisch & Kettenmann, 2007; Yirmiya & Goshen, 2011; Chen & Swanson, 2003). The use of specific radiotracers targeting translocator protein (TSPO), formerly known as peripheral benzodiazepine receptor (PBR) has been broadly utilized in PET evaluation of neuroinflammation (Pannell et al, 2020). PBR is an 18-kDa mitochondrial outer membrane translocator protein, which is widely expressed by many cell types, but in the CNS, it is exclusively localized

in microglia, astrocytes, and macrophages (Pannell et al, 2020; Lavissee et al, 2012; Chen & Guilarte, 2008). While under normal physiological conditions TSPO (PBR) expression in the CNS is minimal, it is highly upregulated during neuroinflammation associated with brain injury and many neurodegenerative conditions (Pannell et al, 2020; Lavissee et al, 2012; Chen & Guilarte, 2008). The TSPO ligand [^{11}C]-peripheral benzodiazepine receptor, [methyl- ^{11}C]N-acetyl-N-(2-methoxybenzyl)-2-phenoxy-5-pyridinamine ([^{11}C]PBR28), has been successfully used as a PET radiotracer for assessing neuroinflammation in rodents (Walker et al, 2015; Mirzaei et al, 2016), non-human primates (Brown et al, 2007; Hannestad et al, 2012), and humans (Kreisl et al, 2009; Alshikho et al, 2018; Sandiego et al, 2015; Toppala et al, 2021; Gershen et al, 2015). [^{18}F] Fluoro-2-deoxy-2-D-glucose [^{18}F] FDG is a glucose analog that is taken up by living cells via cell membrane glucose transporters and subsequently phosphorylated with hexokinase inside most cells; it is not metabolized and does not exit cells. [^{18}F]FDG is a widely used radiotracer for the determination of localized metabolic alterations in the body and has been utilized in the diagnosis and therapy monitoring in various disorders, including cancer, and infectious and inflammatory diseases (Chacko et al, 2017; Glaudemans et al, 2013; Fletcher et al, 2008). PET [^{18}F]FDG imaging is also frequently used to assess brain metabolic activity (Sibson et al, 1998; Rocher et al, 2003; Vo et al, 2014; Uluğ et al, 2011; Vo et al, 2015). In the brain, in addition to neurons, experimental evidence indicates that [^{18}F]FDG PET signal can be driven by astrocytes (Zimmer et al, 2017). It is also documented that microglia increase their metabolic output during inflammation (Baik et al, 2019; Lauro & Limatola, 2020). Therefore, PET [^{18}F]FDG imaging provides information about energy metabolism based on glucose utilization by neurons, astrocytes, and microglia.

We and others have previously shown brain microglial activation, neuroinflammation and metabolic and neurotransmitter system changes in murine models of endotoxemia or cecal ligation and puncture-induced sepsis using invasive and terminal approaches (Silverman et al, 2015; Zaghoul et al, 2017; Hoogland et al, 2015; Qin et al, 2007; Buttini et al, 1996). Here, we investigated the application of dual tracer [^{11}C]PBR28 and [^{18}F]FDG microPET imaging in endotoxemic mice by utilizing an advanced conjunction analysis of the imaging data generated. This methodology involving conjunction analysis provides the advantage of characterizing common brain regions with overlapping neuroinflammatory and metabolic alterations in addition to detecting changes in the brain uptake of each tracer separately. We observed the presence of overlapping increases in radioligand uptake in the hippocampus, the thalamus, and the hypothalamus,

and radiotracer-specific regional alterations, in parallel with increased serum cytokine levels. These observations demonstrate the utility of this dual tracer microPET approach with conjunction analysis to non-invasively examine metabolic activation and neuroinflammation, which have been previously reported in postmortem brain analyses. This methodology can be applied in future studies evaluating brain alterations in preclinical and clinical scenarios.

Methods

Animals

Experiments were performed in accordance with the National Institutes of Health guidelines, and all experimental procedures with animals were approved by the Institutional Animal Care and Use Committee and the Institutional Biosafety Committee of the Feinstein Institutes for Medical Research before humane experimentation. C57BL/6J male mice (13–15 weeks old, Jackson Laboratory) were maintained at room temperature on a 12-h light/dark cycle with free access to food and water.

Endotoxemia

Mice were injected with lipopolysaccharide (LPS, endotoxin) (2 mg/kg, i.p.) ($n=6$) or sterile saline (i.p.) alone as the vehicle control ($n=6$). Six hours after LPS or saline injection mice underwent microPET imaging as described below. In parallel experiments, mice were administered with saline or LPS i.p. and euthanized at the same time point – 6 h, and blood was collected via cardiac puncture and processed for serum cytokine analyses.

MicroPET imaging and analyses

MicroPET imaging was performed using the Inveon® MicroPET imaging system (Siemens) at 6 h post endotoxin or vehicle administration. Briefly, upon arrival to the imaging suite, animals were acclimated for one hour and then anesthetized with 2–2.5% isoflurane mixed in oxygen and the tail vein was cannulated using a 30G custom catheter. [^{18}F]FDG and [^{11}C]PBR28 are routinely synthesized onsite at the PET imaging facility at the Feinstein Institutes and delivered directly into the microPET suite. Approximately 0.5 mCi of [^{11}C]PBR28 (in 0.2 ml) was slowly injected via the tail vein with the simultaneous start of a 60-min dynamic imaging acquisition, followed by a 10-min transmission scan on a Siemens Inveon MicroPET. 1.5 h after the [^{11}C]PBR28 scan, ~0.5 mCi of [^{18}F]FDG (in 0.3 ml) was injected i.p. with 35–40 min allowed for uptake of the tracer followed by a 10 min static scan. Brain images were acquired and reconstructed using Inveon Acquisition workflow (IAW 1.5) and three-dimensional ordered subsets-expectation maximization (3D-OSEM) reconstruction with

attenuation correction. After reconstruction, raw images were bounding box aligned, skull stripped, and dose and weight corrected. [^{18}F]FDG scans from each animal were registered to an [^{18}F]FDG template (Schiffer et al, 2007) and then to a common MRI template (Ma et al, 2005), both of which were aligned within Paxinos and Franklin anatomical space, using Pixel-Wise Modeling (PMOD) 4.0 Software. The rigid transformations from the template-aligned [^{18}F]FDG scans were then applied to the corresponding [^{11}C]PBR28 scans for each animal using statistical parametric mapping (SPM)5 mouse toolbox within MATLAB. Regarding the [^{11}C]PBR28 scan, the final 10 frames of each scan (final 22 mins of dynamic scan) were averaged and used for analysis. Images were smoothed with an isotropic Gaussian kernel FWHM (full width at half maximum) 0.56 mm at all directions.

To identify regions in anatomical space with significant differences between LPS administered and saline administered mice in both [^{18}F]FDG and [^{11}C]PBR28 tracers, we performed whole brain voxel-wise searches with conjunction analysis using SPM-Mouse software (The Wellcome Centre for Human Neuroimaging, UCL Queen Square Institute of Neurology, London, UK, <https://www.fil.ion.ucl.ac.uk/spm/ext/#SPMMouse>) (Sawiak et al, 2009). The conjunction analysis identified the group effects common to the dual tracer, in which the contrasts, testing for a group effect, are specified separately for each tracer. These contrasts are thresholded at a common threshold and combined to give the conjunction. This combination is on a voxel-by-voxel basis, and a new contrast that tests for the conjunction is created. This model was setup with full factorial analysis (2×2) with 2 tracers ([^{18}F]FDG and [^{11}C]PBR28) and 2 groups (LPS and saline). Inter-subject variability in imaging data was accounted for by dividing each PET scan by its global mean value in comparison with the use of cerebellum as a normalization factor. Group differences were considered significant at a voxel-level threshold of $P < 0.005$ for conjunction analysis and $P < 0.001$ for individual analysis with a cluster cutoff of 500 voxels. We identified the significant conjunction clusters, in which both [^{18}F]FDG and [^{11}C]PBR28 values increase or decrease in LPS-administered mice relative to saline-administered mice. We also checked if there are significant clusters, in which values are increased in one tracer and decreased in the other in LPS relative to saline mice or vice versa. We also performed whole brain voxel-wise searches separately for each tracer to validate the results from the conjunction analysis. Individual data from each significant clusters (in Paxinos and Franklin anatomical space) (Paxinos & Franklin, 2019) were identified throughout the whole-brain searches and were measured with post-hoc volume-of-interest (VOI) analyses using in-house MAPLAB

scripts. [^{18}F]FDG and [^{11}C]PBR28 values for the LPS- and saline-treated mice were visualized to evaluate overlapping data and potential outlier effects.

Statistical analysis

All data are presented as the mean \pm SEM. Data analysis was performed using GraphPad Prism software 9.0. Cytokine analysis was performed using the unpaired Mann-Whitney test and $P < 0.05$ was considered significant. In post-hoc analysis of microPET data, values for each significant cluster were similarly compared between the two groups using the unpaired Mann-Whitney test and $P < 0.05$ was considered significant.

Results and discussion

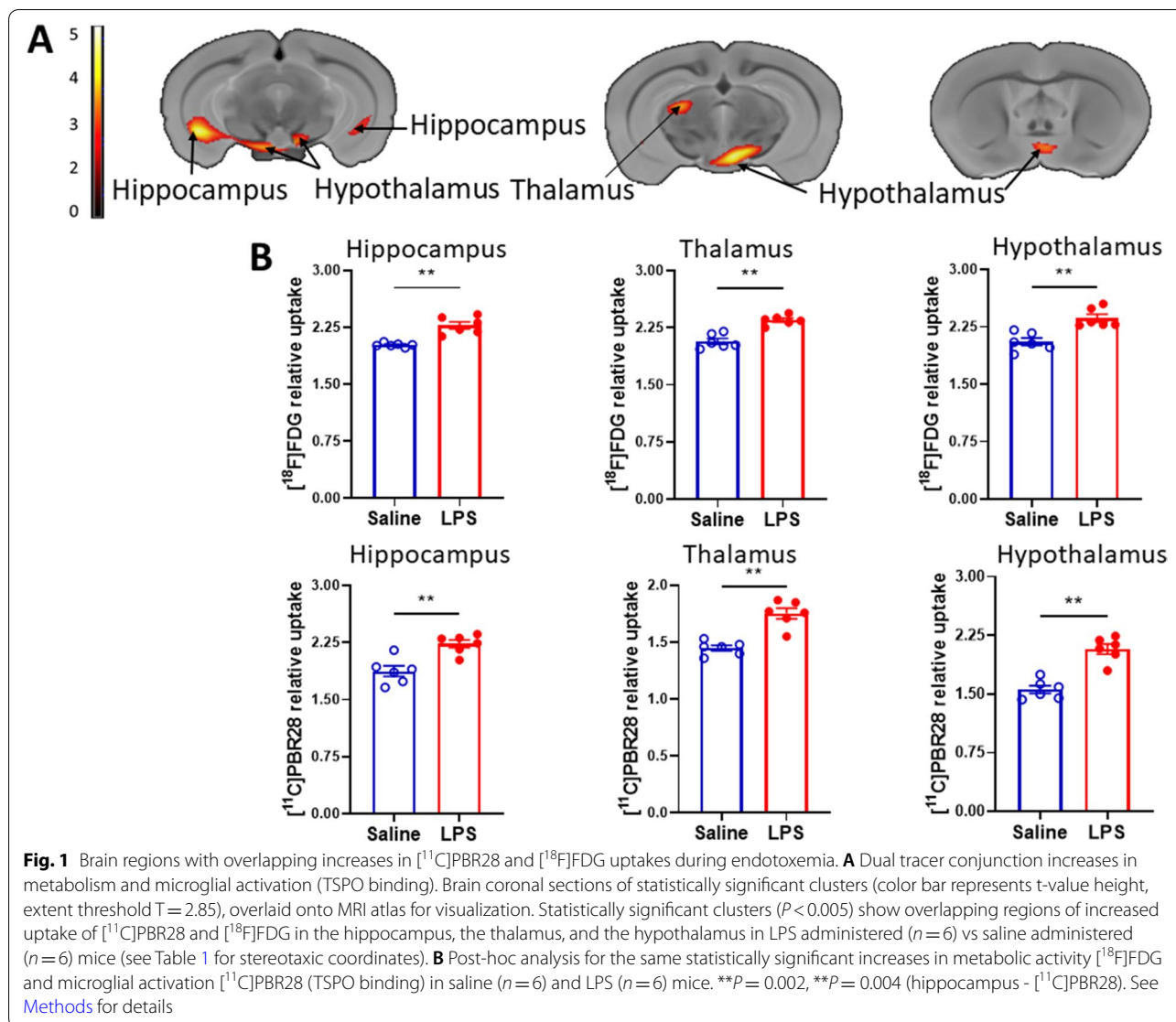
Brain dysfunction including immune and metabolic changes have been described in animals with endotoxemia and CLP sepsis (Silverman et al, 2015; Zaghoul et al, 2017; Hoogland et al, 2015; Qin et al, 2007). We and others have previously shown that peripheral (i.p.) administration of LPS in mice results in neuroinflammatory alterations, including characteristic morphological changes in microglia, indicative of activation in the hippocampus and other brain areas (Silverman et al, 2015; Hoogland et al, 2015; Qin et al, 2007). Here we examined whether neuroinflammation in these brain areas during endotoxemia can be also detected in live mice using a dual tracer microPET imaging subjected to an advanced conjunction analysis. We injected groups of male C57Bl/6 mice with LPS (2 mg/kg) or vehicle (saline) (i.p.) and confirmed the presence of systemic inflammation manifested by significantly increased serum cytokine (TNF, IL-6, IL-1 β , and IL-10) levels at 6 h (Supplementary Fig. 1). Other cohorts of male C57Bl/6 mice were injected with vehicle or the same dose of LPS 6 h prior to acquiring microPET imaging utilizing [^{11}C]PBR28 (~0.5 mCi), followed by [^{18}F]FDG (0.5 mCi) as described in detail in Material and Methods. Applying an advanced conjunction comparative analysis (endotoxemic vs control mice) revealed a significantly increased simultaneous uptake of [^{11}C]PBR28 and [^{18}F]FDG in the hippocampus (Fig. 1A, B) in line with previous immunohistochemical observations showing microglial activation in this brain area (Silverman et al, 2015; Qin et al, 2007). In addition, simultaneous dual tracer uptake increases were observed in the hypothalamus and the thalamus (Fig. 1A, B). The individual analyses of [^{11}C]PBR28 and [^{18}F]FDG uptake (endotoxemic vs saline administered control mice) confirmed increases in each tracer's uptake in the hippocampus, the hypothalamus, and the thalamus (Fig. 2A, B, C, D). In addition, region-specific increases were also observed; [^{18}F]FDG uptake was significantly increased in the cerebellum (Fig. 2A, B), while [^{11}C]PBR28 uptake

was significantly increased in the brainstem (Fig. 2C, D). The SPM conjunction and individual analyses revealed specific patterns of increased brain [^{18}F]FDG and [^{11}C]PBR28 uptake as shown in Table 1. Please include Table 1 here. Applying conjunction analysis also revealed specific decreases in [^{18}F]FDG and [^{11}C]PBR28 uptake in the primary motor and somatosensory cortices (endotoxemic vs control mice) as shown in Fig. 3A, B. These decreases were further confirmed by individual analysis of [^{18}F]FDG and [^{11}C]PBR28 uptake as shown in Supplementary Fig. 2. All results generated using the global mean of normalization were also confirmed using cerebellum value as a reference for normalization (data not shown). These results indicate that peripheral administration of LPS, which causes systemic inflammation manifested by significant increases in circulating cytokine levels, also results in neuroinflammation and brain metabolic alterations, which can be determined using microPET dual tracer imaging.

[^{18}F]FDG and [^{11}C]PBR28 have been previously used together in microPET imaging studies of aortic aneurysm inflammation in rats (English et al, 2014) and β -amyloidosis associated inflammation in lean and obese mice (Barron et al, 2016). However, to the best of our knowledge this study is one of the first to utilize a [^{18}F]FDG and [^{11}C]PBR28 dual tracer imaging combined with a conjunction analysis to assess the impact of peripheral systemic inflammation on the brain.

Microglia are a major cell type with immune function in the CNS/brain and microglial activation drives neuroinflammatory processes (Streit et al, 2004; Borst et al, 2019). Astrocytes are also involved in neuroinflammation (Giovannoni & Quintana, 2020; Chen & Swanson, 2003; Bellaver et al, 2018). There is also a link between microglial activation and induction of a subtype of reactive astrocytes that is mediated through microglial secretion of TNF and other pro-inflammatory molecules (Liddel et al, 2017). This leads to a disruption of the homeostatic relationship between astrocytes and neurons in which astrocytes promote neuronal survival and synaptogenesis, and these reactive astrocytes (designated as A1) induce neuronal death (Liddel et al, 2017).

Brain [^{18}F]FDG uptake determined using PET imaging has been traditionally viewed as a proxy of neuronal activity and its alterations in disease states, including neurodegenerative diseases (Mosconi et al, 2008). However, there is experimental evidence that glucose utilization by astrocytes also determines part of the [^{18}F]FDG PET signal and [^{18}F]FDG PET signal also reflects astrocyte activity (Zimmer et al, 2017). Enhanced [^{18}F]FDG PET signal has been also correlated with microglial activation, for instance in mouse models of Alzheimer's disease (Brendel et al, 2016; Poisnel et al, 2012) and in



experimental neuroinflammatory conditions such as murine amyloidosis (Xiang et al, 2021). Of note, pharmacological depletion of microglia abrogates the increase in $[^{18}\text{F}]\text{FDG}$ uptake in mice with amyloidosis (Xiang et al, 2021). The clinical translatability of these findings was strengthened by observations showing good correlation between microglial activity and $[^{18}\text{F}]\text{FDG}$ uptake determined using PET (Xiang et al, 2021). In view of these previous findings, our results obtained by applying conjunction analysis and individual tracer verification indicate that the increases in $[^{18}\text{F}]\text{FDG}$ and $[^{11}\text{C}]\text{PBR28}$ uptake in the hippocampus, thalamus and hypothalamus reflect brain energy metabolism alterations with neuronal, microglial and astrocytic contributions. This is supported by the individual increases in $[^{18}\text{F}]\text{FDG}$

and $[^{11}\text{C}]\text{PBR28}$ uptake in these brain areas. However, our observation that $[^{11}\text{C}]\text{PBR28}$ uptake is significantly increased in the brainstem (with no $[^{18}\text{F}]\text{FDG}$ uptake increase) indicates the selectivity of this radiotracer for detecting neuroinflammatory responses. In addition, the increased $[^{18}\text{F}]\text{FDG}$ uptake in the cerebellum (with no $[^{11}\text{C}]\text{PBR28}$ uptake increase) suggests an increased metabolic activity most likely driven by neuronal signaling with no significant microglial contribution. The differential impact of systemic inflammation on the brain was indicated by the observed simultaneous and individual decreases in $[^{18}\text{F}]\text{FDG}$ and $[^{11}\text{C}]\text{PBR28}$ uptake in the primary motor and somatosensory cortices. Intriguingly, in addition to suppressed neuronal activity, these findings indicate a process of suppressed microglial activity. This

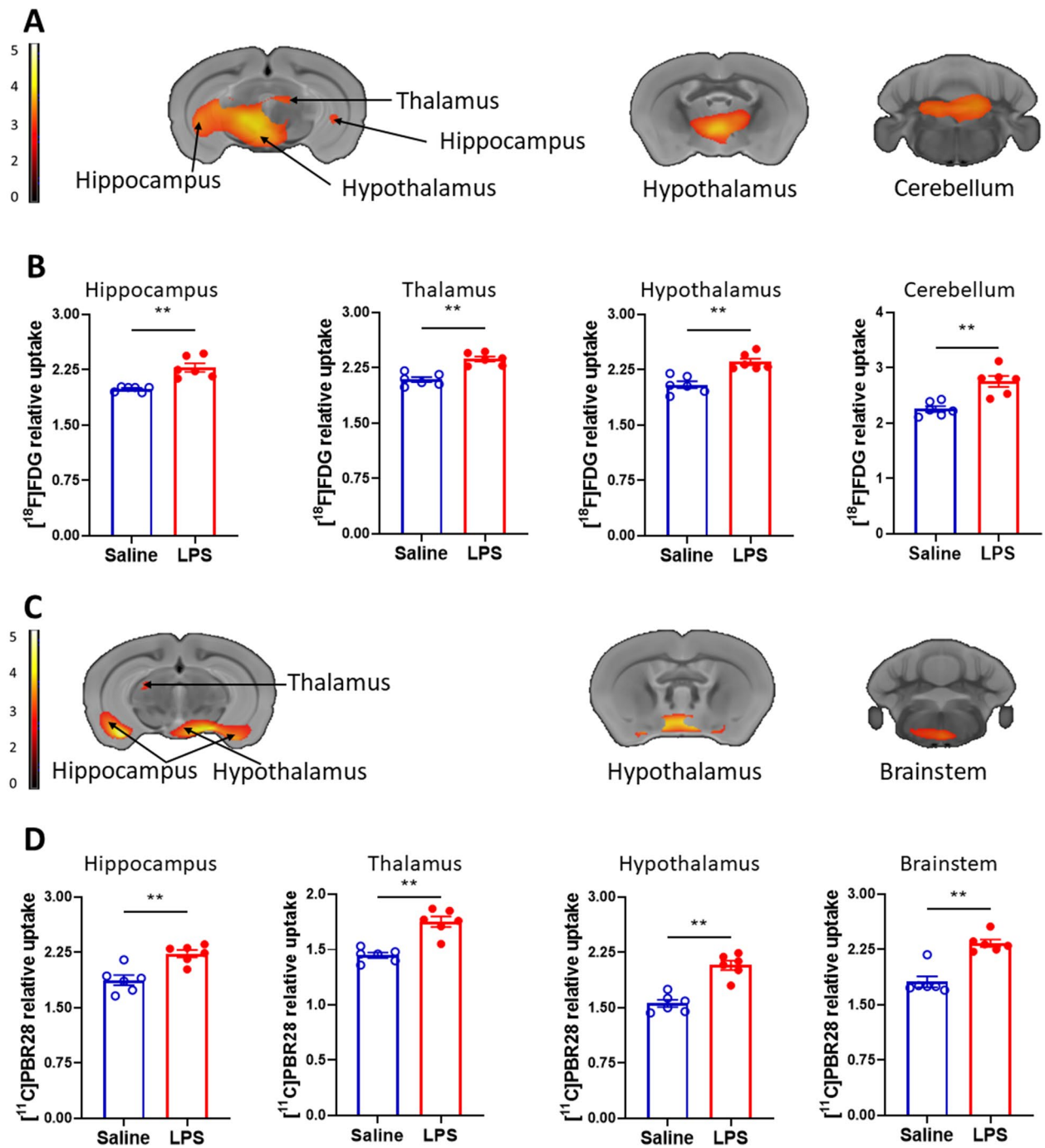


Fig. 2 Brain regions with individual increases in $[^{11}\text{C}]\text{PBR28}$ and $[^{18}\text{F}]\text{FDG}$ uptake during endotoxemia. **A** Increased $[^{18}\text{F}]\text{FDG}$ uptake in the hippocampus, the thalamus, the hypothalamus, and the cerebellum shown in coronal sections in LPS administered ($n=6$) vs saline administered ($n=6$) mice (see Table 1 for specific stereotaxic coordinates). SPM clusters (color bar represents t-value height, cutoff threshold $T=3.55$) overlaid onto MRI atlas for visualization. Statistically significant clusters ($P<0.001$). **B** Post-hoc analysis of $[^{18}\text{F}]\text{FDG}$ tracer uptake in the same groups (saline, $n=6$ and LPS, $n=6$) of mice. $**P=0.002$. **C** Increased $[^{11}\text{C}]\text{PBR28}$ metabolic activity in the hippocampus, the thalamus, the hypothalamus, and the brainstem shown in coronal sections in LPS administered ($n=6$) vs saline administered ($n=6$) mice (see Table 1 for stereotaxic coordinates). SPM clusters (color bar represents t-value height, cutoff threshold $T=3.55$). Statistically significant clusters ($P<0.001$) overlaid onto MRI atlas for visualization. **D** Post-hoc analysis of $[^{11}\text{C}]\text{PBR28}$ uptake in the same groups (saline, $n=6$ and LPS, $n=6$) of mice. $**P=0.002$, $**P=0.004$ (hippocampus). See [Methods](#) for details

Table 1 Specific brain regions with significant [¹⁸F]FDG and [¹¹C]PBR28 uptake increases*

Radiotracer/Brain region	Brain coordinates**			Relative radiotracer uptake (controls) (mean ± SD)	Relative radiotracer uptake (LPS) (mean ± SD)
	X (mm)	Y (mm)	Z (mm)		
Dual [¹⁸ F]FDG and [¹¹ C]PBR28 uptake					
Paraventricular hypothalamus anterior parvicellular	0.2	−0.5	−4.5	[¹⁸ F]FDG = 2.06 ± 0.11 [¹¹ C]PBR28 = 1.56 ± 0.11	[¹⁸ F]FDG = 2.36 ± 0.11 [¹¹ C]PBR28 = 2.07 ± 0.14
CA1 Hippocampus pyramidal cell layer	−3.3	−3.5	−4.1	[¹⁸ F]FDG = 2.02 ± 0.03	[¹⁸ F]FDG = 2.28 ± 0.10
CA1 Hippocampus pyramidal cell layer	3.4	−3.3	−4.0	[¹¹ C]PBR28 = 1.87 ± 0.15	[¹¹ C]PBR28 = 2.23 ± 0.11
LP Thalamic nucleus laterocaudal	−1.9	−2.8	−2.6	[¹⁸ F]FDG = 2.07 ± 0.08 [¹¹ C]PBR28 = 1.45 ± 0.05	[¹⁸ F]FDG = 2.34 ± 0.06 [¹¹ C]PBR28 = 1.75 ± 0.11
[¹⁸ F]FDG uptake					
Glomerular layer olfactory	0.0 0.0 −0.2	4.4 5.2 5.5	−2.9 −3.4 −2.8	2.14 ± 0.10	2.71 ± 0.26
Periaqueductal grey	−2.3	−2.8	−2.9	2.12 ± 0.07	2.50 ± 0.21
CA1 Pyramidal layer hippocampus	3.3	−3.0	−3.4	1.99 ± 0.03	2.28 ± 0.13
Red nucleus parvicell part	−0.6	−3.2	−3.8	2.29 ± 0.21	2.83 ± 0.14
Posterior thalamic nucleus	−1.0	−3.4	−3.4	2.09 ± 0.08	2.37 ± 0.07
[¹¹ C]PBR28 uptake					
Tuberal region lateral hypothalamus	0.9	−0.9	−5.2	1.56 ± 0.11	2.07 ± 0.14
Medial amygdalar nucleus posterodorsal	1.8	−1.4	−5.2	1.85 ± 0.10	2.34 ± 0.10
Parasubthalamic nucleus	1.3	−2.1	−5.0	1.45 ± 0.05	1.75 ± 0.11
Caudomedial entorhinal	3.5 3.2	−5.1 −5.1	−4.1 −4.6	1.87 ± 0.15	2.23 ± 0.11

*Increased tracer uptake was identified using statistical parametric mapping (SPM5) with $P < 0.005$ in the conjunction analysis and $P < 0.001$ in the individual tracer uptake analysis (with an extent threshold of $t = 500$ voxels), comparing saline administered mice ($n = 6$) vs LPS administered mice ($n = 6$)

**According to (Paxinos & Franklin, 2019), X (Mediolateral), Y (Anteroposterior), Z (Dorsoventral)

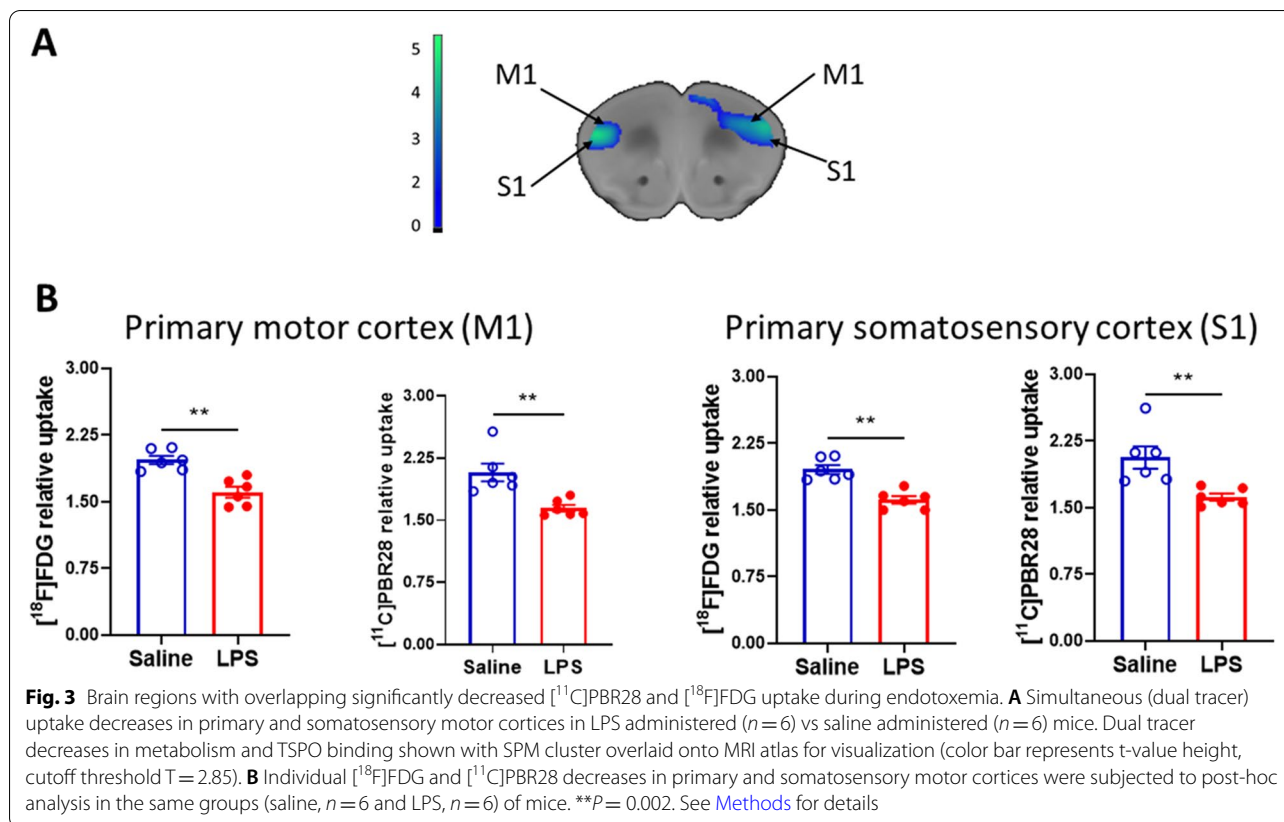
observation is driven at least in part by the use of normalized radiotracer uptake in the analysis and deserves future examination in terms of its neurobiological interpretation and implication.

Of note, there is recent evidence for the presence of TSPO in brain vascular endothelial cells, cerebellar Purkinje cells, and neural stem/progenitor cells, indicating a broader range of cell populations expressing TSPO in the normal mouse brain (Betlazar et al, 2018). However, the contribution of these cellular sources of TSPO to the brain [¹¹C]PBR28 uptake in the absence and presence of inflammation is presently unknown.

There are a few possible mechanisms underlying the impact of systemic inflammation on the brain (Pavlov & Tracey, 2015; Silverman et al, 2015; Pavlov et al, 2018; Capuron & Miller, 2011). In endotoxemia, direct activation of neuroinflammation by LPS is unlikely because of poor LPS penetration across the blood–brain barrier (Qin et al, 2007). However, pro-inflammatory cytokines, including TNF, IL-1b, and IL-6, whose circulating levels were significantly elevated have a demonstrated role in immune cell activation in the brain (Qin et al, 2007; Nadeau & Rivest, 1999). Very recently, a key role for TNF and TNF-STAT signaling was shown in astrocytic

dysfunction and blood brain barrier impairment (Kim et al, n.d.). Underlying events may involve cytokine crossing of the blood–brain barrier by a saturable carrier-mediated mechanism, binding receptors at the surface of the endothelium of brain capillaries with the release of soluble mediators, such as prostaglandins and nitric oxide or acting via circumventricular organs that lack blood–brain barrier function (Qin et al, 2007; Capuron & Miller, 2011; Nadeau & Rivest, 1999; Pavlov et al, 2003). The expression of TLR4 and cytokine receptors on microglia and astrocytes provide a triggering mechanism for neuroinflammatory responses.

There is some skepticism about the clinical relevance of evaluating microglial activation using single tracer PET imaging, such as [¹¹C]PBR28. As recently summarized, in Alzheimer's disease, multiple sclerosis and amyotrophic lateral sclerosis increased [¹¹C]PBR28 uptake is most likely a result of increased number of microglia rather than increased activation (Nutma et al, n.d.). Therefore, a dual or multi-tracer studies involving [¹⁸F]FDG and [¹¹C]PBR28, and/or other specific ligands, capable of capturing alterations in the energy metabolism and the functional state of microglial activation may provide more complete evaluation.



The time point of our study microPET imaging study, i.e., 6h after LPS administration was chosen based on data from previous postmortem studies demonstrating microglial activation and neuroinflammation at early stages of endotoxemia. The single time point could be considered as a limitation of our study. Further investigations evaluating brain region specific patterns of dual tracer uptake increases or decreases will be necessary to provide a more detailed characterization of brain alterations at different stages of endotoxemia.

The brain regulation of physiological functions is key to homeostasis. The hippocampus has a major role in the regulation of memory. The hypothalamus is an important regulator of the brain autonomic outflow that regulates several peripheral functions and its integration with the neuroendocrine regulation of physiological processes. The thalamus is a key region associated with processing sensory information. Further, the brainstem - the most evolutionarily conserved region of the brain - provides integrated reflex regulation of numerous physiological processes, including inflammation. Recently, it was demonstrated that a brainstem nucleus - the dorsal motor nucleus of the vagus controls peripheral TNF release through the vagus nerve-mediated *inflammatory reflex* (Kressel et al, 2020). The

cerebellum contributes to motor and nonmotor functions, adaptive plasticity, and cognition. The primary somatosensory (S1) and primary motor (M1) cortices are reciprocally connected, and their interaction contribute to coordinated motor output. Changes in energy metabolism and neuroinflammation in these brain areas may result in cognitive impairment and other brain functional alterations. These changes may also lead to compromised regulations of peripheral physiological processes, which are specifically attributed to these brain areas. Thus, while systemic inflammation has an impact on the brain, in turn, altered brain function may contribute to and exacerbate peripheral pathology.

Conclusions

Our observations indicate that neuroinflammatory alterations in endotoxemic mice, previously demonstrated utilizing postmortem evaluation (Silverman et al, 2015; Hoogland et al, 2015) can be reliably detected using dual tracer non-invasive microPET imaging. It is important to note that our observations reflect changes in the brain at early stages of endotoxemia and different patterns of brain alterations can be expected at later stages. These findings are of interest for further PET-based non-invasive evaluation of neuroinflammation in preclinical

models and clinical settings of sepsis, and other lethal and debilitating disorders characterized by peripheral immune and metabolic dysregulation.

Abbreviations

(¹¹C)PBR28: [¹¹C]-peripheral benzodiazepine receptor, [methyl-¹¹C]N-acetyl-N-(2-methoxybenzyl)-2-phenoxy-5-pyridinamine; CNS: Central nervous system; [¹⁸F]FDG: [¹⁸F] Fluoro-2-deoxy-2-D-glucose; IAW: Inveon Acquisition workflow; LPS: Lipopolysaccharide; microPET: Micro positron emission tomography; PMOD: Pixel-Wise Modeling; 3D-OSEM: Three-dimensional ordered subsets-expectation maximization; TSPO: Translocator protein..

Supplementary Information

The online version contains supplementary material available at <https://doi.org/10.1186/s42234-022-00101-2>.

Additional file 1: Supplementary Fig. 1. LPS administration results in significant increases in serum cytokine levels. Mice were injected with saline ($n=8$) or LPS (2 mg/kg, i.p.) ($n=6$) and euthanized 6h later. Blood was obtained through cardiac puncture and cytokines analyzed in the serum (** $P=0.0007$). See [Methods](#) for details.

Additional file 2: Supplementary Fig. 2. Brain individual tracer uptake decreases. Statistically significant clusters ($P<0.001$) of individual [¹⁸F]FDG and [¹¹C]PBR28 decreases in primary and somatosensory motor cortices were subjected to post-hoc analysis of decreases in the same groups (saline, $n=6$ and LPS, $n=6$) of mice. ** $P=0.002$; *** $P=0.007$ ([¹⁸F]FDG - M1). See [Methods](#) for details.

Additional file 3: Supplementary methods. Serum cytokines analysis. Cytokines, including TNF, IL-6, IL-10, and IL-1b, were determined in serum using a cytokine panel detection kit (Invitrogen) following the manufacturer's recommendations.

Acknowledgements

Not applicable.

Authors' contributions

VAP, JC, YM, and EHC conceived the project. VAP, JC, YM, and EHC designed experiments. SP, JC, LT, HL, TT, and DH performed experiments. JC, AV, YM, SP, and AF analyzed data. All authors discussed the results and commented on the manuscript. VAP, JC, and YM wrote the manuscript. All other authors reviewed the manuscript and provided comments. All authors read and approved the final manuscript.

Funding

This work was supported by the National Institutes of Health (NIH), National Institute of General Medical Sciences Grants: R01GM128008 and R01GM121102 (to VAP) and 1R35GM118182 (to KJT).

Availability of data and materials

All data generated are included in this article and its supplementary information files. The datasets analyzed during the current study are available from the corresponding author on reasonable request.

Declarations

Ethics approval and consent to participate

Not applicable.

Consent for publication

Not applicable.

Competing interests

The authors declare no competing interests.

Author details

¹The Feinstein Institutes for Medical Research, Northwell Health, Manhasset, NY, USA. ²Donald and Barbara Zucker School of Medicine at Hofstra/Northwell, Hempstead, NY, USA.

Received: 18 October 2022 Accepted: 9 November 2022

Published online: 30 November 2022

References

- Alshikho MJ, Zürcher NR, Loggia ML, Cernasov P, Reynolds B, Pijanowski O, et al. Integrated magnetic resonance imaging and [(11)C]-PBR28 positron emission tomographic imaging in amyotrophic lateral sclerosis. *Ann Neurol*. 2018;83(6):1186–97.
- Baik SH, Kang S, Lee W, Choi H, Chung S, Kim J-I, et al. A breakdown in metabolic reprogramming causes microglia dysfunction in Alzheimer's disease. *Cell Metab*. 2019;30(3):493–507.e6.
- Barron AM, Tokunaga M, Zhang MR, Ji B, Suhara T, Higuchi M. Assessment of neuroinflammation in a mouse model of obesity and β -amyloidosis using PET. *J Neuroinflammation*. 2016;13(1):221.
- Bellaver B, dos Santos JP, Leffa DT, Bobermin LD, Roppa PHA, da Silva Torres IL, et al. Systemic inflammation as a driver of brain injury: the astrocyte as an emerging player. *Mol Neurobiol*. 2018;55(3):2685–95.
- Betlazar C, Harrison-Brown M, Middleton RJ, Banati R, Liu GJ. Cellular sources and regional variations in the expression of the Neuroinflammatory marker translocator protein (TSPO) in the Normal brain. *Int J Mol Sci*. 2018;19(9):2707.
- Brendel M, Probst F, Jaworska A, Overhoff F, Korzhova V, Albert NL, et al. Glial activation and glucose metabolism in a transgenic amyloid mouse model: a triple-tracer PET study. *J Nucl Med*. 2016;57(6):954–60.
- Brown AK, Fujita M, Fujimura Y, Liow JS, Stabin M, Ryu YH, et al. Radiation dosimetry and biodistribution in monkey and man of 11C-PBR28: a PET radioligand to image inflammation. *J Nucl Med*. 2007;48(12):2072–9.
- Borst K, Schwabenland M, Prinz M. Microglia metabolism in health and disease. *Neurochem Int*. 2019;130:104331.
- Buras JA, Holzmann B, Sitkovsky M. Animal models of sepsis: setting the stage. *Nat Rev Drug Discov*. 2005;4(10):854–65.
- Buttini M, Limonta S, Boddeke HW. Peripheral administration of lipopolysaccharide induces activation of microglial cells in rat brain. *Neurochem Int*. 1996;29(1):25–35.
- Capuron L, Miller AH. Immune system to brain signaling: neuropsychopharmacological implications. *Pharmacol Ther*. 2011;130(2):226–38.
- Chen M-K, Guilarte TR. Translocator protein 18 kDa (TSPO): molecular sensor of brain injury and repair. *Pharmacol Ther*. 2008;118(1):1–17.
- Chen Y, Swanson RA. Astrocytes and brain injury. *J Cereb Blood Flow Metab*. 2003;23(2):137–49.
- Chacko AM, Watanabe S, Herr KJ, Kalimuddin S, Tham JY, Ong J, et al. 18F-FDG as an inflammation biomarker for imaging dengue virus infection and treatment response. *JCI insight*. 2017;2(9).
- English SJ, Diaz JA, Shao X, Gordon D, Bevard M, Su G, et al. Utility of (18)F-FDG and (11)C-PBR28 microPET for the assessment of rat aortic aneurysm inflammation. *EJNMMI Res*. 2014;4(1):20.
- Fletcher JW, Djulbegovic B, Soares HP, Siegel BA, Lowe VJ, Lyman GH, et al. Recommendations on the use of 18F-FDG PET in oncology. *J Nucl Med*. 2008;49(3):480–508.
- Garden GA, Möller T. Microglia biology in health and disease. *J Neuroimmune Pharmacol*. 2006;1(2):127–37.
- Gershen LD, Zanotti-Fregonara P, Dustin IH, Liow JS, Hirvonen J, Kreisler WC, et al. Neuroinflammation in temporal lobe epilepsy measured using positron emission tomographic imaging of translocator protein. *JAMA neurology*. 2015;72(8):882–8.
- Giovannoni F, Quintana FJ. The role of astrocytes in CNS inflammation. *Trends Immunol*. 2020;41(9):805–19.
- Glaudemans AW, de Vries EF, Galli F, Dierckx RA, Slart RH, Signore A. The use of (18)F-FDG-PET/CT for diagnosis and treatment monitoring of inflammatory and infectious diseases. *Clin Dev Immunol*. 2013;2013:623036.
- Gofton TE, Young GB. Sepsis-associated encephalopathy. *Nat Rev Neurol*. 2012;8(10):557–66.
- Hanisch UK, Kettenmann H. Microglia: active sensor and versatile effector cells in the normal and pathologic brain. *Nat Neurosci*. 2007;10(11):1387–94.

- Hannestad J, Gallezot JD, Schafbauer T, Lim K, Kloczynski T, Morris ED, et al. Endotoxin-induced systemic inflammation activates microglia: [¹¹C]PBR28 positron emission tomography in nonhuman primates. *Neuroimage*. 2012;63(1):232–9.
- Heneka MT, Carson MJ, El Khoury J, Landreth GE, Brosseron F, Feinstein DL, et al. Neuroinflammation in Alzheimer's disease. *Lancet Neurol*. 2015;14(4):388–405.
- Hoogland IC, Houbolt C, van Westerloo DJ, van Gool WA, van de Beek D. Systemic inflammation and microglial activation: systematic review of animal experiments. *J Neuroinflammation*. 2015;12:114.
- Kreisl WC, Mbeo G, Fujita M, Zoghbi SS, Pike VW, Innis RB, et al. Stroke incidentally identified using improved positron emission tomography for microglial activation. *Arch Neurol*. 2009;66(10):1288–9.
- Kressel AM, Tsaava T, Levine YA, Chang EH, Addorisio ME, Chang Q, et al. Identification of a brainstem locus that inhibits tumor necrosis factor. *Proc Natl Acad Sci U S A*. 2020;117(47):29803–10.
- Kim H, Leng K, Park J, Sorets AG, Kim S, Shostak A, et al. Reactive astrocytes transduce blood-brain barrier dysfunction through a TNF α -STAT3 signaling axis and secretion of alpha 1-antichymotrypsin. *bioRxiv*. 2022:2022.02.21.481336.
- Lauro C, Limatola C. Metabolic reprogramming of microglia in the regulation of the innate inflammatory response. *Front Immunol*. 2020;11:493.
- Lavisse S, Guillemier M, Hérard AS, Petit F, Delahaye M, Van Camp N, et al. Reactive astrocytes overexpress TSP0 and are detected by TSP0 positron emission tomography imaging. *J Neurosci*. 2012;32(32):10809–18.
- Leng F, Edison P. Neuroinflammation and microglial activation in Alzheimer disease: where do we go from here? *Nat Rev Neurol*. 2021;17(3):157–72.
- Liddel SA, Guttenplan KA, Clarke LE, Bennett FC, Bohlen CJ, Schirmer L, et al. Neurotoxic reactive astrocytes are induced by activated microglia. *Nature*. 2017;541(7638):481–7.
- Ma Y, Hof PR, Grant SC, Blackband SJ, Bennett R, Slatost L, et al. A three-dimensional digital atlas database of the adult C57BL/6J mouse brain by magnetic resonance microscopy. *Neuroscience*. 2005;135(4):1203–15.
- Meneses G, Cárdenas G, Espinosa A, Rassy D, Pérez-Osorio IN, Bárcena B, et al. Sepsis: developing new alternatives to reduce neuroinflammation and attenuate brain injury. *Ann N Y Acad Sci*. 2019;1437(1):43–56.
- Metz CN, Pavlov VA. Treating disorders across the lifespan by modulating cholinergic signaling with galantamine. *J Neurochem*. 2021;158(6):1359–80.
- Mirzaei N, Tang SP, Ashworth S, Coello C, Plisson C, Passchier J, et al. In vivo imaging of microglial activation by positron emission tomography with [(11)C]PBR28 in the 5XFAD model of Alzheimer's disease. *Glia*. 2016;64(6):993–1006.
- Mosconi L, Tsui WH, Herholz K, Pupi A, Drzezga A, Lucignani G, et al. Multicenter standardized 18F-FDG PET diagnosis of mild cognitive impairment, Alzheimer's disease, and other dementias. *J Nucl Med*. 2008;49(3):390–8.
- Nadeau S, Rivest S. Effects of circulating tumor necrosis factor on the neuronal activity and expression of the genes encoding the tumor necrosis factor receptors (p55 and p75) in the rat brain: a view from the blood-brain barrier. *Neuroscience*. 1999;93:1449–64.
- Nutma E, Fancy N, Weinert M, Marzin MC, Tsartsalis S, Muirhead RCJ, et al. Translocator protein is a marker of activated microglia in rodent models but not human neurodegenerative diseases. *bioRxiv*. 2022:2022.05.11.491453.
- Pannell M, Economopoulos V, Wilson TC, Kersemans V, Isenegger PG, Larkin JR, et al. Imaging of translocator protein upregulation is selective for pro-inflammatory polarized astrocytes and microglia. *Glia*. 2020;68(2):280–97.
- Patel PN, Shah RY, Ferguson JF, Reilly MP. Human experimental Endotoxemia in modeling the pathophysiology, genomics, and therapeutics of innate immunity in complex Cardiometabolic diseases. *Arterioscler Thromb Vasc Biol*. 2015;35(3):525–34.
- Pavlov VA, Tracey KJ. Neural circuitry and immunity. *Immunol Res*. 2015;63(1–3):38–57.
- Pavlov VA, Wang H, Czura CJ, Friedman SG, Tracey KJ. The cholinergic anti-inflammatory pathway: a missing link in neuroimmunomodulation. *Mol Med*. 2003;9(5–8):125–34.
- Pavlov VA, Chavan SS, Tracey KJ. Molecular and functional neuroscience in immunity. *Annu Rev Immunol*. 2018;36:783–812.
- Pavlov VA, Tracey KJ. Bioelectronic medicine: preclinical insights and clinical advances. *Neuron*. 2022;110(21):3627–44.
- Paxinos G, Franklin KB. Paxinos and Franklin's the mouse brain in stereotaxic coordinates. Academic press; 2019.
- Poisnel G, Herard A-S, El Tayara NET, Bourrin E, Volk A, Kober F, et al. Increased regional cerebral glucose uptake in an APP/PS1 model of Alzheimer's disease. *Neurobiol Aging*. 2012;33(9):1995–2005.
- Qin L, Wu X, Block ML, Liu Y, Breese GR, Hong J-S, et al. Systemic LPS causes chronic neuroinflammation and progressive neurodegeneration. *Glia*. 2007;55(5):453–62.
- Rocher AB, Chapon F, Blaizot X, Baron JC, Chavoix C. Resting-state brain glucose utilization as measured by PET is directly related to regional synaptophysin levels: a study in baboons. *Neuroimage*. 2003;20(3):1894–8.
- Sandiego CM, Gallezot JD, Pittman B, Nabulsi N, Lim K, Lin SF, et al. Imaging robust microglial activation after lipopolysaccharide administration in humans with PET. *Proc Natl Acad Sci U S A*. 2015;112(40):12468–73.
- Sawiak SJ, Wood NI, Williams GB, Morton AJ, Carpenter TA. Voxel-based morphometry in the R6/2 transgenic mouse reveals differences between genotypes not seen with manual 2D morphometry. *Neurobiol Dis*. 2009;33(1):20–7.
- Schiffer WK, Mirrione MM, Dewey SL. Optimizing experimental protocols for quantitative behavioral imaging with ¹⁸F-FDG in rodents. *J Nucl Med*. 2007;48(2):277–87.
- Sibson NR, Dhankhar A, Mason GF, Rothman DL, Behar KL, Shulman RG. Stoichiometric coupling of brain glucose metabolism and glutamatergic neuronal activity. *Proc Natl Acad Sci U S A*. 1998;95(1):316–21.
- Silverman HA, Dancho M, Regnier-Golanov A, Nasim M, Ochanin M, Olofsson PS, et al. Brain region-specific alterations in the gene expression of cytokines, immune cell markers and cholinergic system components during peripheral endotoxin-induced inflammation. *Mol Med*. 2015;20:601–11.
- Singer M, Deutschman CS, Seymour CW, Shankar-Hari M, Annane D, Bauer M, et al. The third international consensus definitions for Sepsis and septic shock (Sepsis-3). *Jama*. 2016;315(8):801–10.
- Sprung CL, Peduzzi PN, Shatney CH, Schein RM, Wilson MF, Sheagren JN, et al. Impact of encephalopathy on mortality in the sepsis syndrome. The veterans administration systemic Sepsis cooperative study group. *Crit Care Med*. 1990;18(8):801–6.
- Streit WJ, Mrak RE, Griffin WST. Microglia and neuroinflammation: a pathological perspective. *J Neuroinflammation*. 2004;1(1):14.
- Toppala S, Ekblad LL, Tuisku J, Helin S, Johansson JJ, Laine H, et al. Association of Early β -amyloid accumulation and Neuroinflammation measured with [(11)C]PBR28 in elderly individuals without dementia. *Neurology*. 2021;96(12):e1608–e19.
- Uluğ AM, Vo A, Argyelan M, Tanabe L, Schiffer WK, Dewey S, et al. Cerebellar thalamocortical pathway abnormalities in torsinA DYT1 knock-in mice. *Proc Natl Acad Sci U S A*. 2011;108(16):6638–43.
- Vo A, Volpe BT, Tang CC, Schiffer WK, Kowal C, Huerta PT, et al. Regional brain metabolism in a murine systemic lupus erythematosus model. *J Cereb Blood Flow Metab*. 2014;34(8):1315–20.
- Vo A, Sako W, Dewey SL, Eidelberg D, Uluğ AM. 18FDG-microPET and MR DTI findings in Tor1a+/- heterozygous knock-out mice. *Neurobiol Dis*. 2015;73:399–406.
- Walker MD, Dinelle K, Kornelsen R, Lee NV, Miao Q, Adam M, et al. [(11)C]PBR28 PET imaging is sensitive to neuroinflammation in the aged rat. *J Cereb Blood Flow Metab*. 2015;35(8):1331–8.
- Xiang X, Wind K, Wiedemann T, Blume T, Shi Y, Briel N, et al. Microglial activation states drive glucose uptake and FDG-PET alterations in neurodegenerative diseases. *Sci Transl Med*. 2021;13(615):eabe5640.
- Yirmiya R, Goshen I. Immune modulation of learning, memory, neural plasticity and neurogenesis. *Brain Behav Immun*. 2011;25(2):181–213.
- Zaghloul N, Addorisio ME, Silverman HA, Patel HL, Valdes-Ferrer SI, Ayasolla KR, et al. Forebrain cholinergic dysfunction and systemic and brain inflammation in murine Sepsis survivors. *Front Immunol*. 2017;8:1673.
- Zimmer ER, Parent MJ, Souza DG, Leuzy A, Lecrux C, Kim H-I, et al. [18F]FDG PET signal is driven by astroglial glutamate transport. *Nat Neurosci*. 2017;20(3):393–5.

Publisher's Note

Springer Nature remains neutral with regard to jurisdictional claims in published maps and institutional affiliations.